Viscosity of water measured to pressures of 6 GPa and temperatures of 300 °C

Evan H. Abramson
Department of Earth and Space Sciences, University of Washington, Seattle, Washington 98195, USA
(Received 2 August 2007; published 21 November 2007)

Shear viscosities of fluid water have been measured to 300 °C and 6 GPa (60 kbar). Measurements were made in a diamond-anvil cell with a rolling-ball technique. Enskog's equation for viscosity, coupled with an *ad hoc* assumption that increased collision rates are due to an "excluded volume", yield excellent matches to the data at temperatures of 100 °C and over, without any freely variable parameter. The data overlap the pressure-temperature range in which experiments on shocked water have previously been interpreted to indicate extremely high viscosities. It is shown conclusively that viscosities in this region are very close to those at ambient temperature. Further, it is argued that explanations of high apparent viscosities which rely on the putative formation of ice behind the shock front are probably incorrect.

DOI: 10.1103/PhysRevE.76.051203 PACS number(s): 66.20.+d, 62.50.+p, 61.20.Gy

I. INTRODUCTION

The shear viscosities of highly compressed fluids are important to the studies of planetary physics, explosive materials, and high pressure chemistry as well as to the basic theory of fluids. Nonetheless, due to the difficulty of the experiments there have been relatively few reports of viscosities at pressures in excess of ~0.5 GPa. Water, as a ubiquitous substance of great practical and theoretical importance, has engendered more attention in this regard than any other fluid, but still the data are sparse. Water's viscosity under static compression has previously been reported to ~1 GPa and less than 100 °C by Bridgman [1], Forst *et al.* [2], Bett and Cappi [3,4], Harlow [5], and King [6]. Other measurements by Dudziak and Franck [7], up to a temperature of 560 °C, have extended only to 0.35 GPa.

Several methods have been used to infer the viscosities of water transiently compressed by shocks, to a maximum pressure of 25 GPa and associated temperature of ~1700 K. Some researchers have concluded that the viscosities of such shocked water can exceed that of the normal fluid by as much as six orders of magnitude. Results of various experiments, however, differ by the same six orders of magnitude, indicating that proper interpretations of the data have not yet been established.

In this paper we report measurements of the viscosity of water in the fluid and metastable fluid regimes up to a temperature of 300 °C and a pressure of 6 GPa (60 kbar). The data are used to test several, previously published, empirical and semiempirical equations. The pressures and temperatures of these experiments overlap those of the shock data and demonstrate conclusively that water's viscosity in this regime is normal, varying little from ambient values.

II. EXPERIMENT

Water was held in a high-pressure diamond-anvil cell of modified Merrill-Basset design. Viscosities were determined with a rolling-ball technique [6,8] in which a videocamera is used to record the speed of a platinum sphere as it rolls down an inner diamond face of the cell. Spheres were of diameters between 30 and 60 μm. The plane of roll was inclined at angles of between 10° and 30° from the horizontal. Plots of speed versus sine of the angle yielded straight lines, the slopes of which are inversely proportional to the viscosities. The constant of proportionality for each sphere is dependent on the diameter and was calculated from the known viscosities of water at 21 °C (and pressures less than 0.5 GPa) given by the International Association for the Properties of Water and Steam (IAPWS) [9,10]. Figure 1 shows a plot of speed against angle of inclination for two different spheres at similar pressures; note that although the larger sphere rolls faster than the smaller for any given angle, the calculated viscosities are the same.

The cell was held in an oven, with temperatures measured and regulated to 1 °C using chromel-alumel thermocouples. Pressures were measured with an included crystal of either ruby [11] or samarium-doped SrB_4O_7 [12,13]; for the borate, or for ruby above 200 °C, the pressure gauge was separated from the working water by means of a gold divider [13].

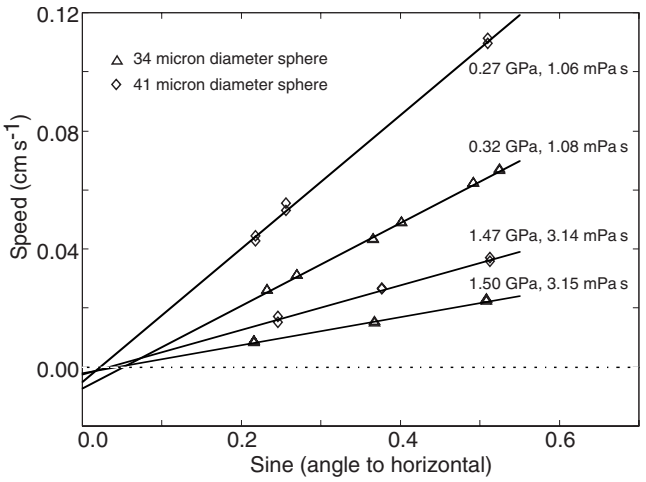

FIG. 1. Rolling speeds, measured in water at 21 °C, are plotted against sine of the angle to the horizontal. Data are presented for two spheres of different diameter, at similar low and high pressures. Under identical conditions the larger sphere rolls roughly twice as fast as the smaller, but calculated viscosities, given in the figure, are the same.

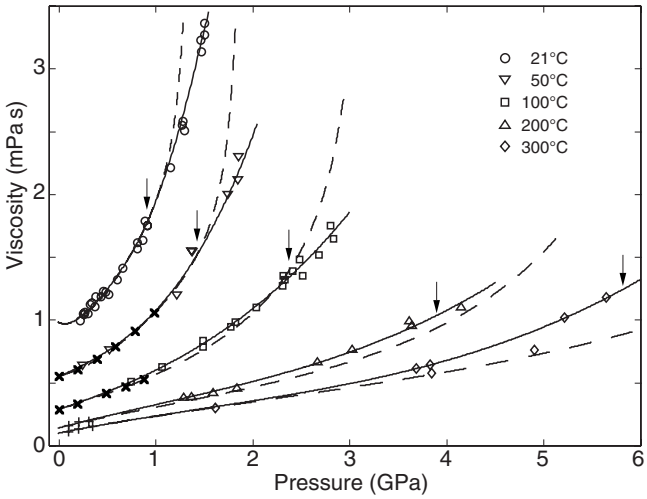

FIG. 2. Measured viscosities are plotted against pressure along isotherms of 21, 50, 100, 200 and 300 °C. Data of Cappi [3,4] (×) and of Dudziak and Franck [7] (+) are also shown. Solid lines are polynomial fits through the data, dotted lines represent calculations of Aleksandrov and Matveev [15]. Arrows indicate the freezing pressure on each isotherm.

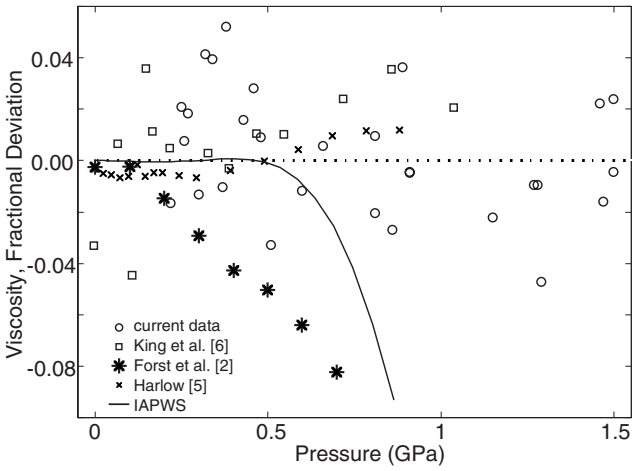

FIG. 3. Measured viscosities are plotted against pressure as fractional deviations from a smooth curve drawn through the current 21 °C data. ○, current data; ×, Harlow [5]; ∗, Forst *et al.* [2]; □ King *et al.* [6] (for 2 wt % NaCl solution); and solid line, IAPWS formulation [9,10]. All data were taken at 21±2 °C and are corrected to 21 °C. Data of Cappi are not reproduced here as they were taken in the same laboratory as those of Harlow and are much the same. As originally published, the data of King *et al.* were calibrated against a single point taken at 1 bar. Here, the reported viscosities have been uniformly reduced by 4% to better match other data up to 0.5 GPa.

Reynolds numbers ranged from 2×10^{-3} to 1.0 with no obvious onset of turbulent or non-Newtonian flow.

III. RESULTS AND DISCUSSION

A. Data

Data [14] were taken on isotherms of 21, 50, 100, 200, and 300 °C (Fig. 2). Overall, the agreement with previous results is quite good within the regions of overlap. Deviations from a smooth curve drawn through our 21 °C data are shown in Fig. 3; individual measurements have a root-mean-square scatter of ~3%. In the same figure are plotted results from previous experiments. Data taken with conventional high pressure apparatus have typically used either falling plugs or rolling spheres moving through cylinders of slightly larger diameters; these measurements often show precisions of better than 1%, but at pressures approaching 1 GPa can deviate on the order of 10% among different laboratories. Such systematic offsets have been reasonably ascribed to dimensional changes in the apparatus caused by the large pressures [2]. In the case of the current technique dimensional changes due to pressure or temperature are believed to be inconsequential, a belief supported by the fact that repeated measurements with spheres and cells of different dimensions are seen to yield the same viscosities (Fig. 1).

Along the isotherms up to 200 °C it was relatively easy to push the fluid ~0.4 GPa into the metastable regime with respect to either ice VI (<82 °C) or ice VII. Viscosities in the metastable fluid show no obvious departure from the regular increase with pressure seen in the thermodynamically stable region.

The IAPWS formulation, depicted along the 21 °C isotherm in Fig. 3, was not designed with the purpose of extrapolation and diverges quickly beyond the region of fitted data. Aleksandrov and Matveev developed equations [15] intended to be useful in extrapolation (stippled lines, Fig. 2) which do reasonably well in reproducing much of the data, with the notable exception of the metastable regime for which they predict divergent viscosities at the highest densities achieved.

B. Commonly used fitting equations

Several expressions are commonly used for the purpose of describing the variation of viscosity with pressure, temperature, or density. The Doolittle [16] equation $\eta\propto e^{B\rho/(\rho-\rho_0)}$, found to give decent fits to viscosities for many liquids, also does so for (liquid) water at or over 100 °C (although, notably, not the 21 or 50 °C isotherms). The range of densities of the present data put no great demand on a three-parameter expression and the most that can be said is that the fitting constants obtained are reasonable. A modified Doolittle expression, shown [8] to fit oxygen viscosities from the thin gas to liquid densities, is not useful for water at these temperatures which are still below critical (and for which, moreover, the second viscosity virial coefficient is negative).

The Arrhenius relations, $\eta\propto e^{E_a/kT}$ and $\eta\propto e^{PV_a/kT}$, with constant energy or volume of activation (E_a and V_a, respectively) are often used when it is desired to extrapolate or interpolate viscosities. These equations fit neither the current data nor those previously taken for oxygen [8], either along isobars or isotherms and it seems doubtful that they should be used at all unless for interpolative purposes and where sufficient intermediate points exist that the data can be shown to conform to the equation. This fact, which is well-known among those studying glassing [17], appears to be less widely appreciated in other fields.

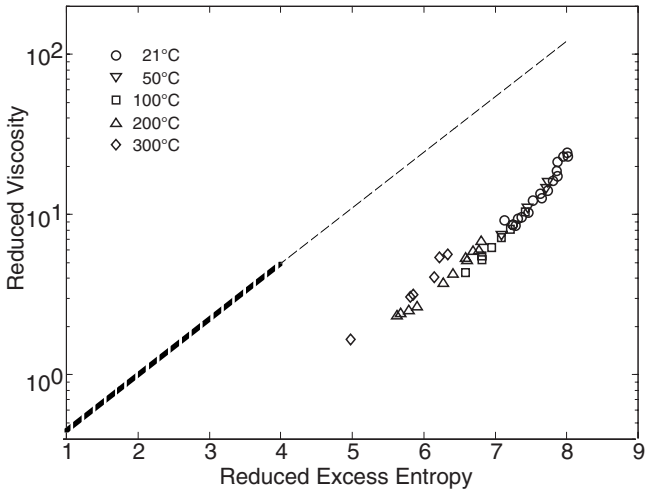

FIG. 4. Reduced viscosity is plotted against (negative) reduced excess entropy [Eq. (1)]. The dashed line is an approximation [19] to molecular dynamics (MD) calculations for structureless particles; the thicker segment denotes the range of the MD results.

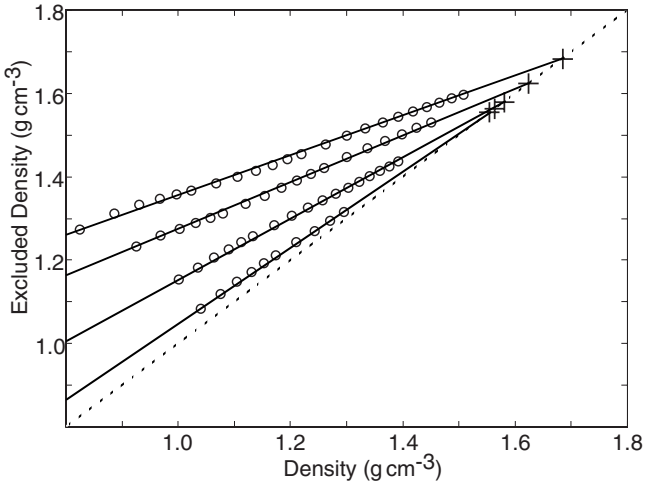

FIG. 5. Excluded density (inverse excluded volume) as calculated by Eq. (3) is plotted against fluid density for isotherms of 21, 100, 200, and 300 °C (bottom to top). Crosses give the densities of ice VII on the melting line at these temperatures. Straight lines are interpolations between the measured data point at lowest pressure (0.1 GPa) and the point at which the excluded density equals that of ice VII. In conjunction with Eq. (3) the lines are used to calculate the curves in Fig. 6.

The Vogel-Fulcher-Tammann equation $\eta \propto e^{DT_0/(T-T_0)}$ gives a decent account of the data to within 1% up to 1.5 GPa (fits were not attempted at higher pressures with fewer isotherms). Its superiority to the Arrhenius expression might be explained solely by the addition of a third fitting parameter, however, it is notable that the values obtained for T_0 are a good match to the temperatures at which high-density amorphous (HDA) ice is seen to devitrify.

C. Reduced entropy correlation

Computer simulations of ensembles of structureless particles, with a variety of model potentials, suggest [18,19] an exponential relation between a reduced viscosity and a reduced excess entropy:

$$\eta_{\mathrm{red}} = \eta\rho^{-2/3}/(mkT)^{1/2},$$

$$s = -(S - S_{\mathrm{ideal\ gas}})/Nk: \quad \eta_{\mathrm{red}} = ae^{bs}, \tag{1}$$

with a $\sim$0.2 and b $\sim$0.8; such a connection would be of tremendous value as the entropy is a well-defined and measurable quantity. Figure 4 shows a rough organization of the data along these lines, but shifted significantly in entropy and with a decided curvature. The shift is approximately that which would be expected if the vibrational contribution to the fluid's entropy were equal to that of the gas while the rotational contribution was halved. Data taken at 1 bar [20–22] show a more pronounced curvature toward higher viscosities as the fluid becomes deeply supercooled.

D. Excluded volume

Hard-sphere models in general and Enskog theory in particular have been the starting points for many attempts at modeling transport properties and are quite successful at low to intermediate ($\sim$ twice critical) densities [23]. Application to real systems requires a procedure for determining the effective hard sphere diameters and much thought has been directed to this problem [23,24], especially to deriving hard sphere diameters from thermodynamic data.

In Enskog's formulation, the viscosity is given by

$$\eta = \eta_0/\chi + 5/(16\sigma^2)\sqrt{mkT/\pi}[0.8b\rho + 0.761(b\rho)^2\chi], \tag{2}$$

where $b = 2\pi\sigma^3/3$, η_0 is the viscosity at zero density, and σ is the hard-sphere (collisional) diameter. The factor χ accounts for the increased collision rate (over that of a structureless fluid of point particles) due to local ordering and for hard spheres it is taken as the value of the pair distribution function at the sphere's diameter. Lyusternik [25] has pointed out that if one makes an *ad hoc* interpretation of the increased collision rate as the result of an "excluded volume" V_e, with $\chi = V/(V - V_e)$, and further that V_e is proportional to the volume of the supposed hard sphere $V_e = (1/f)(\pi\sigma^3/6)$, then the Enskog equation for viscosity can be recast in terms of V_e as [26]

$$\eta = \eta_0(V - V_e)/V + (5/16)\sqrt{mkT/\pi}[\pi/(6fV_e)]^{2/3} \times [3.2fV_e/V + 12.18(fV_e)^2/V/(V - V_e)]. \tag{3}$$

All this only becomes interesting when one realizes that $1/V_e$, calculated for known viscosities and plotted against density (Fig. 5), yields approximations to straight lines. Further, these lines when extended pass close to the points $\rho = 1/V_e = 1/V_{\mathrm{iceVII}}$ where V_{iceVII} is the volume [27] of ice VII at the melting pressure [28] on that isotherm. As a predictive prescription, we may then approximate $1/V_e$ by a straight line drawn through a single point at some low density with known viscosity, and the point $\rho = \rho_{\mathrm{iceVII}}$, allowing us to interpolate V_e and hence η at intermediate points. Viscosities thus obtained are shown in Fig. 6. For purposes of this cal-

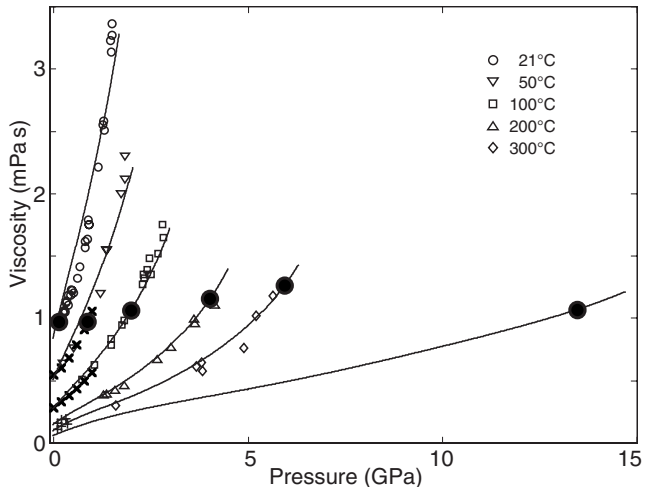

FIG. 6. Experimentally determined viscosities are plotted against pressure along several isotherms. Curves are extrapolated from known viscosities at 0.1 GPa through use of Eq. (3) in conjunction with the straight lines of Fig. 5; the curve extending to 15 GPa is drawn for a temperature of 1000 K. A solid circle is drawn on each isotherm at the calculated [13] pressure of the shock Hugoniot; viscosities of shocked water are seen to remain remarkably constant, in accord with the results of Hamman and Linton (see Fig. 7).

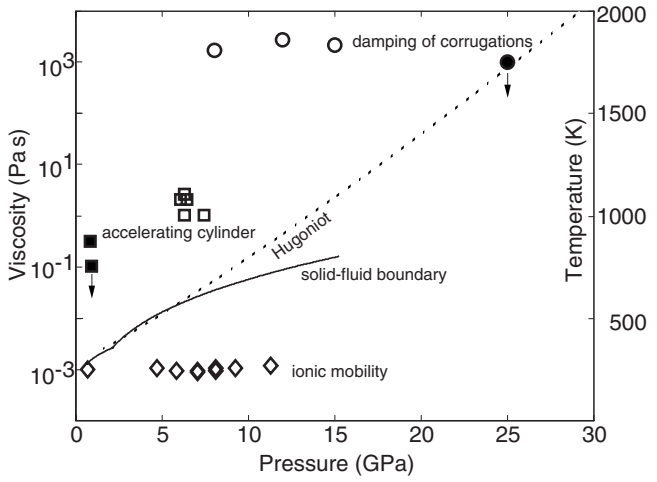

FIG. 7. Measured viscosities (log scale given on left side of graph) are plotted against shock pressure for several different experiments. Solid squares, Al'tshuler *et al.* [35], accelerating cylinder; open squares, Kim [34], accelerating cylinder; solid circle, Mineev and Savinov [33], damped corrugations; open circles, Mineev and Zaidel [32], damped corrugations; and diamonds, Hamann and Linton [36,37], ionic conductance. Solid symbols indicate that the data only provide upper bounds on the viscosities. Also shown are calculated temperatures (scale given on right side of graph) of shocked water (stippled line) and the melting curve of water (solid line) [28]; water ends up in the stability field of ice VII only between shock pressures of ~3 and 5.5 GPa.

culation the factor f has been taken to be 0.35, appropriate [29] to a fluid locally arranged as an fcc lattice with spacing just small enough to confine each molecule in the cage of its 12 neighbors, however, the value chosen has little effect on the final calculated viscosities.

At various temperatures below 82 °C four different polymorphs of ice (Ih, III, V, and VI) lie along the melting curve of water. In this range, where the thermodynamically favored form of packing for water may be presumed to be shifting rapidly, the calculated viscosities fail to match the data. Beyond 82 °C ice VII becomes the stable modification and persists as such up to approximately 700 °C (and, perhaps, 35–45 GPa) [30,31]. Correspondingly the prescription gives an excellent account of the data along the 100, 200, and 300 °C isotherms.

In the face of all the preceding approximations and assumptions, I wish to emphasize the absence of free parameters in the final results. It is this fact only, coupled with the surprisingly good match between measured and predicted viscosities (Fig. 6), that gives reason to suppose that the development contains some essentially correct physics which deserve to be further explored.

E. Shocked water

The use of shocks to transiently compress materials to high densities and temperatures is long-established and reasonably well-understood. Multiple and varied attempts to measure the viscosities of shock-compressed water have led to reported values differing by up to six orders of magnitude (Fig. 7). Observations of the damping of induced corrugations [32,33], and others of the acceleration of entrained metallic cylinders [34,35], have been interpreted as indications of viscosities which increase greatly with pressure, to (depending on the experiment) 1 or 1000 Pa s in the pressure range of 6–15 GPa. On the other hand, Hamman and Linton [36,37] found no change in the electrical conductivities of aqueous ionic solutions which were shocked up to pressures of 14 GPa; assuming an approximate inverse correlation between viscosity and ionic mobility (Walden's rule), they then deduced that the viscosities of the shocked solutions were not significantly different from those under ambient conditions. The huge discrepancies among these various experiments have not yet been satisfactorily resolved.

In an attempt to reconcile these discordant results, several authors have suggested [33,35,38,39] that extreme increases in apparent viscosity are due to the formation of solid water in a span of pressure for which the shock Hugoniot (locus of shock end points) exists within the region of stability of ice VII. Partial solidification of the fluid would be expected to increase the effective viscosity as measured on the macroscopic scale while producing little change in the mobility of ions through the remaining (connected) fluid. A related idea [35] supposes that the water, although not containing actual crystalline bodies, does contain large, highly hydrogen-bonded "flow units" which hinder macroscopic movement while, again, allowing essentially unimpeded movement of ions.

It is clear from the current data that, at least on the lower end of the pressures and temperatures previously established by the shocks, viscosities of the thermally equilibrated *fluid* are similar to those at ambient conditions; there is no development of tightly bonded "flow units" or strong "precrystallization effects" near the melting line, a conclusion

also apparent, *a fortiori*, from data taken in the metastable regions. Use of Eq. (3) to estimate viscosities at higher temperatures and pressures than yet measured statically further emphasizes the relative invariance of the viscosity along the Hugoniot (Fig. 6). Both the experimental data as well as the extrapolations agree quite well with the conclusions of Hamman and Linton; taken together they provide an interesting validation of Walden's rule, over large compressions (densities of $1-1.7\ \mathrm{g\ cm^{-3}}$) and over temperatures ranging from 300 to 1000 K.

The idea that the presence of ice may cause the large purported viscosities seems based mainly on the proximity of the Hugoniot to the melt line, coupled with the absence of other acceptable explanations. Direct experimental support for the formation of ice is poor and derives almost entirely from an early paper [40] in which a diminution in transparency behind the shock front was reported (along with a possible abrupt change in slope of the Hugoniot which might also be indicative of phase transition). In a later paper Kormer [41] found no evidence of reduced transparency after a single shock and, in retrospect, the sparse data with large scatter can be reasonably fitted with a smooth curve. Recent work by Dolan and Gupta [42] indicates that water which is multiply (quasi-isentropically) shocked to 5 GPa, and thus deeply into the stability field of ice VII, freezes only through inhomogeneous nucleation on particular substrates; over the course of the experiments, which lasted $\sim 1\ \mu$s, homogeneous nucleation was never observed. Measurements of viscosity in shocks, using either accelerated cylinders or the damping of corrugations, were complete within a few microseconds after passage of the shock front. It seems unlikely that ice could have formed soon enough, in sufficient quantity, to affect the impressed corrugations, although it might nucleate about the accelerated cylinders.

Whether ice can form at all depends upon the location of the Hugoniot with respect to the melt line; this, due mostly to uncertainty in the position of the Hugoniot, is a matter of disagreement. The locus of shocked states is fairly well-known in the coordinates P-ρ-E, but the temperatures are inferred through the use of various more or (very often) less reasonable approximations to the thermodynamics. Figure 7 shows our calculation of the temperatures of water (shocked from an initial state of 20 °C and 1 bar), using an equation of state [13] based on measured speeds of sound as well as shock data taken in this pressure range. The figure indicates that while ice might be able to form between 3 and 5 GPa, it will not exist stably at higher shock pressures.

IV. CONCLUSIONS

The shear viscosity of water has been measured up to 300 °C and ~6 GPa. The data are in accord with previous measurements which extended to 1 GPa. The highest viscosities measured, ~3.3 mPa s, were in room temperature water driven into a metastable state; at higher pressures the concomitant increased temperatures necessary to avoid solidification caused the viscosities to be uniformly lower.

The viscosities of fluid water remain unequivocally close to the ambient value (1 mPa s) along the primary shock Hugoniot up to 6 GPa. Extrapolation by use of Eq. (3) up to 1000 K and 13.5 GPa also yields a viscosity of 1 mPa s, in good agreement with the data of Hamann and Linton; Walden's rule is thus verified. The reported extreme viscosities of shocked water are not credibly explained by positing the formation of ice as this contradicts the available thermodynamic and kinetic data.

A prescription based on Enskog's equation for hard spheres coupled with a hypothesized "excluded volume" gives a surprisingly good account of the data between 100 and 300 °C without recourse to any free parameters. A suggested relation between scaled viscosity and excess entropy suffers, in application to a real molecular system, from effects of internal degrees of freedom. Still, when plotted against the excess entropy, the scaled viscosities group along a line parallel to that given by simulations using structureless particles.

ACKNOWLEDGMENTS

Design of the apparatus and subsequent data collection were undertaken with the able help of H. West-Foyle. This work was supported by the U.S. Dept. of Energy, Contract No. DE-FG52-06NA26214.

[1] P. W. Bridgman, Proc. Am. Acad. Arts Sci. **61**, 57 (1926).
[2] P. Forst, F. Werner, and A. Delgado, Rheol. Acta **39**, 566 (2000).
[3] K. E. Bett and J. B. Cappi, Nature (London) **207**, 620 (1965).
[4] J. B. Cappi, Ph.D. thesis, Imperial College of Science and Technology, 1964 (unpublished).
[5] A. Harlow, Ph.D. thesis, Imperial College of Science and Technology, 1967 (unpublished).
[6] H. E. King Jr., E. Herbolzheimer, and R. L. Cook, J. Appl. Phys. **71**, 2071 (1992).
[7] K. H. Dudziak and E. U. Franck, Ber. Bunsenges. Phys. Chem. **70**, 1120 (1966).
[8] E. H. Abramson, J. Chem. Phys. **122**, 84501 (2005).
[9] J. T. R. Watson, R. S. Basu, and J. V. Sengers, J. Phys. Chem. Ref. Data **9**, 1255 (1980).
[10] J. V. Sengers and J. T. R. Watson, J. Phys. Chem. Ref. Data **15**, 1291 (1986).
[11] H. K. Mao, J. Xu, and P. M. Bell, J. Geophys. Res. **91**, 4673 (1986).
[12] F. Datchi, R. LeToullec, and P. Loubeyre, J. Appl. Phys. **81**, 3333 (1997).
[13] E. H. Abramson and J. M. Brown, Geochim. Cosmochim. Acta **68**, 1827 (2004).
[14] See EPAPS Document No. E-PLEEE8-76-194710 for a table of measured viscosities. For more information on EPAPS, see http://www.aip.org/pubservs/epaps.html.

[15] A. A. Aleksandrov and A. B. Matveev, Teplofiz. Vys. Temp. **36**, 719 (1998) [High Temp. **36**, 695 (1998)]; **36**, 908 (1998) [High Temp. **36**, 885 (1998)].
[16] A. K. Doolittle, J. Appl. Phys. **22**, 1471 (1951).
[17] C. A. Angell, Chem. Rev. (Washington, D.C.) **102**, 2627 (2002).
[18] R. Grover, W. G. Hoover, and B. Moran, J. Chem. Phys. **83**, 1255 (1985).
[19] Y. Rosenfeld, Phys. Rev. A **15**, 2545 (1977).
[20] J. Hallett, Proc. Phys. Soc. London **82**, 1046 (1963).
[21] Y. A. Osipov, B. V. Zheleznyi, and N. F. Bondarenko, Zh. Fiz. Khim. **51**, 1264 (1977) [Russ. J. Phys. Chem. **51**, 1264 (1977)].
[22] E. H. Trinh and K. Ohsaka, Int. J. Thermophys. **16**, 545 (1995).
[23] H. J. M. Hanley, R. D. McCarty, and E. G. D. Cohen, Physica (Amsterdam) **60**, 322 (1972).
[24] S. Bastea, Phys. Rev. E **68**, 031204 (2003).
[25] V. E. Lyusternik, Teplofiz. Vys. Temp. **28**, 686 (1990) [High Temp. **28**, 509 (1990)].
[26] The equation as originally published suffers from typographical errors and a cursory description; this is a reconstruction.
[27] Y. Fei, H.-K. Mao, and R. J. Hemley, J. Chem. Phys. **99**, 5369 (1993).
[28] F. Datchi, P. Loubeyre, and R. LeToullec, Phys. Rev. B **61**, 6535 (2000).
[29] R. J. Buehler, R. H. Wentorf, Jr., O. Hirschfelder, and C. F. Curtiss, J. Chem. Phys. **19**, 61 (1951).
[30] A. F. Goncharov, N. Goldman, L. E. Fried, J. C. Crowhurst, I. Feng, W. Kuo, C. J. Mundy, and J. M. Zaug, Phys. Rev. Lett. **94**, 125508 (2005).
[31] J.-F. Lin *et al.*, Geophys. Res. Lett. **32**, L11306 (2005).
[32] V. N. Mineev and R. M. Zaidel, Zh. Eksp. Teor. Fiz. **54**, 1633 (1968) [Sov. Phys. JETP **27**, 874 (1968)].
[33] V. N. Mineev and E. V. Savinov, Zh. Eksp. Teor. Fiz. **68**, 1321 (1975) [Sov. Phys. JETP **41**, 656 (1976)].
[34] G. K. Kim, Prikl. Mekh. Tekh. Fiz. **25**, 44 (1984) [J. Appl. Mech. Tech. Phys. **25**, 692 (1984)].
[35] L. V. Al'tshuler, G. S. Doronin, and G. K. Kim, Prikl. Mekh. Tekh. Fiz. **27**, 110 (1986) [J. Appl. Mech. Tech. Phys. **27**, 887 (1986)].
[36] S. D. Hamann and M. Linton, J. Appl. Phys. **40**, 913 (1969).
[37] S. D. Hamann and M. Linton, Trans. Faraday Soc. **62**, 2186 (1969).
[38] G. H. Miller and T. J. Ahrens, Rev. Mod. Phys. **63**, 919 (1991).
[39] V. N. Mineev and A. I. Funtikov, Teplofiz. Vys. Temp. **43**, 136 (2005) [High Temp. **43**, 141 (2005)].
[40] L. V. Al'tshuler, A. A. Bakanova, and R. F. Trunin, Dokl. Akad. Nauk SSSR **121**, 67 (1958) [Sov. Phys. Dokl. **3**, 761 (1958)].
[41] S. B. Kormer, K. B. Yushko, and G. V. Krishkevich, Zh. Eksp. Teor. Fiz. **54**, 1640 (1968) [Sov. Phys. JETP **54**, 1640 (1968)].
[42] D. H. Dolan and Y. M. Gupta, J. Chem. Phys. **121**, 9050 (2004).